Theory of Acoustic Breathing Modes of Core−Shell Nanoparticles

J. E. Sader,[†] G. V. Hartland,[‡] and P. Mulvaney*[,§]

Department of Mathematics and Statistics, The University of Melbourne, Victoria, 3010, Australia, Department of Chemistry and Biochemistry, University of Notre Dame, Indiana 46556-5670, and School of Chemistry, The University of Melbourne, Victoria, 3010, Australia

Received: November 6, 2001

Recent experiments by Hodak et al. [*J. Phys. Chem. B* **2000**, *104*, 5053] on core−shell nanoparticles have demonstrated that the frequency of the breathing mode is strongly dependent on the shell thickness. Here we compare these measurements with a theoretical model based on classical continuum mechanics, which in itself includes a model for the kinetics of shell formation. It is found that the experimental measurements can be modeled accurately using this theoretical approach. This finding will facilitate the control and characterization of the mechanical properties of core−shell nanoparticles.

Introduction

Over the last two decades, considerable interest has focused on the synthesis of quantum dots and small metal crystallites. In particular, the optical, magnetic and electrical properties of small particles have been intensively investigated. However, an understanding of fundamental material properties such as melting point, Young's modulus, and shear modulus will be essential if these particles are to be employed in nanoscale devices, motors, or electronics. A vexed issue is establishing how one can probe mechanical properties such as compressibility or density, which appear to require manual contact with the materials. For small semiconductor crystals at least, it has been shown that the acoustic phonon modes are quantized, and the phonon frequency depends on the speed of sound in the particles. Thus, examining the acoustic phonon modes provides a means of investigating the elastic properties of these particles.[1]

Recently, Hodak et al.[2,3] demonstrated that laser excitation of small gold particles coherently excites the acoustic vibrational modes, as the photon energy absorbed by the particles is impulsively transferred to the ionic lattice. These oscillations were found to correspond to the zeroth-order acoustic mode or breathing motion of the particles. The resultant breathing mode frequencies ω (in rad/sec) were found to be extremely well described by the classical formula for a homogeneous, elastic sphere with a free surface, first derived by Lamb in 1882:[4]

$$\omega = \frac{\tau\alpha}{a} \tag{1}$$

where a is the radius of the particle and τ is the smallest positive root of the eigenvalue equation $\tau \cot \tau = 1 - \tau^2/4\kappa^2$, where $\kappa = \beta/\alpha$ is the ratio of the transverse β and longitudinal α speeds of sound in the material. Interestingly, bulk material values for α and β were used in all cases examined in refs 2 and 3, which encompassed gold particles ranging in diameter from 8 to 120 nm. Excellent agreement between eq 1 and experimental measurement was found throughout.

In many cases, however, nanoparticles are synthesized as core−shell structures. For example, semiconductor core−shell structures can be used to trap excited-state charge carriers within the photoexcited core, which results in enhanced band edge luminescence from the core particle.[5] Particles may also be coated with silica to enhance colloid stability and processability,[6] while metal−metal core−shell particles are often synthesized as a means to modulate the position of the surface plasmon band of the core.[7] Therefore, it is likely that in many cases, photon energy will eventually lead to the pumping of energy into the acoustic modes of small, coated spheres. This was demonstrated recently by Hodak et al.,[8] who measured the vibration frequencies for lead coated gold nanoparticles. No comparison with theory was made in ref 8, where it was commented that a suitable theory for core−shell nanoparticles does not exist at present. It is the principal aim of this paper to demonstrate that the vibration of metal core−shell nanoparticles can be accurately described using a theoretical model derived under continuum assumptions, which are identical to those used to derive eq 1. This in turn will enable the accurate characterization, design, and control of the mechanical properties of core−shell nanoparticles.

Theory

The theoretical analysis of the core−shell nanoparticle experiment will consist of two distinct parts. First, we shall analyze the vibration of a core−shell particle, presenting the general theoretical framework and explicit analytical expressions for the vibrational frequency as a function of the material properties and dimensions of the particle. Second, we shall theoretically investigate the experimental shell formation process performed in ref 8. This will enable us to give an a priori estimate for the thickness of the shell, which we find is slightly lower than that predicted in ref 8.

Core−Shell Particle. We focus our attention on the acoustic breathing mode of a core−shell spherical particle, with core radius a_{core} and shell thickness Δ. It is assumed that the core and shell are both composed of homogeneous, isotropic, linearly elastic materials, and both are consequently modeled as continua; i.e., the molecular structure of the core and shell are ignored. Since we are interested in the breathing modes only, we investigate the radial oscillation of the sphere. We therefore

* Corresponding author. E-mail: mulvaney@unimelb.edu.au.
[†] Department of Mathematics and Statistics, The University of Melbourne. E-mail: jsader@unimelb.edu.au.
[‡] Department of Chemistry and Biochemistry, University of Notre Dame. E-mail: hartland.1@nd.edu.
[§] School of Chemistry, The University of Melbourne.

10.1021/jp014068s CCC: $22.00
Published on Web 01/19/2002

search for radial oscillations of the form

$$u(r,t) = U(r)\exp(i\omega t) \tag{2}$$

where u is the radial displacement of the sphere, r is the radial distance from the center of the sphere, ω is the radial frequency, and t is time. In a homogeneous medium, the function U satisfies[9]

$$\frac{d^2U}{dr^2} + \frac{2}{r}\frac{dU}{dr} - \frac{2}{r^2}U + h^2U = 0 \tag{3}$$

where $h = \omega/\alpha$ and α is the longitudinal speed of sound in the material. Solving eq 3 in the core and the shell then gives the following general expressions for the displacement U in each region:

$$U_{core}(r) = A\left(\frac{\cos(h_{core}r)}{h_{core}r} - \frac{\sin(h_{core}r)}{(h_{core}r)^2}\right) \tag{4a}$$

$$U_{shell}(r) = B\left(\frac{\cos(h_{shell}r)}{(h_{shell}r)^2} + \frac{\sin(h_{shell}r)}{h_{shell}r}\right) + C\left(\frac{\cos(h_{shell}r)}{h_{shell}r} - \frac{\sin(h_{shell}r)}{(h_{shell}r)^2}\right) \tag{4b}$$

where A, B, and C are constants to be determined, and

$$h_{core} = \frac{\omega}{\alpha_{core}}, \qquad h_{shell} = \frac{\omega}{\alpha_{shell}} \tag{5}$$

where the subscripts "core" and "shell" henceforth refer to values in the core and shell, respectively. To find A, B, and C, we apply the appropriate boundary conditions at the core−shell interface and the outer shell surface. We note that the displacement and normal stress must be continuous at the core−shell interface, and the normal stress is zero at the outer shell surface.[10] This gives the following boundary conditions:

$$[U_{core} = U_{shell}]_{r=a_{core}} \tag{6a}$$

$$\left[\frac{dU_{core}}{dr} + 2(1-2\kappa_{core}^2)\frac{U_{core}}{r} = \lambda\left(\frac{dU_{shell}}{dr} + 2(1-2\kappa_{shell}^2)\frac{U_{shell}}{r}\right)\right]_{r=a_{core}} \tag{6b}$$

$$\left[\frac{dU_{shell}}{dr} + 2(1-2\kappa_{shell}^2)\frac{U_{shell}}{r}\right]_{r=a_{core}} + \Delta = 0 \tag{6c}$$

where

$$\kappa = \frac{\beta}{\alpha} \tag{7a}$$

$$\lambda = \frac{\rho_{shell}\alpha_{shell}^2}{\rho_{core}\alpha_{core}^2} \tag{7b}$$

where ρ is the density of the material. Substituting eq 4 into 6 then results in an eigenvalue equation for the breathing mode frequency ω. Unfortunately, the resulting expression is highly complex, and therefore, the complete expression is not presented here. We note, however, that when $\Delta/a_{core} = 0$ or ∞, a homogeneous sphere is obtained, and we recover the original expression derived by Lamb, eq 1, as expected. In addition, explicit analytical formulas can be obtained by performing an asymptotic expansion of the eigenvalue equation in cases where the shell thickness Δ is small or large in comparison to the core radius a_{core}. This results in the following formulas for the natural resonant frequency ω:

$$\omega = \frac{\alpha_{core}\tau_{core}}{a_{core}}\left\{1 - A_{core}\left(\frac{\Delta}{a_{core}}\right) + O\left(\left(\frac{\Delta}{a_{core}}\right)^2\right)\right\}, \qquad \frac{\Delta}{a_{core}} \ll 1 \tag{8a}$$

$$\omega = \frac{\alpha_{shell}\tau_{shell}}{a_{core}+\Delta}\left\{1 + A_{shell}\left(\frac{a_{core}}{a_{core}+\Delta}\right)^3 + O\left(\left(\frac{a_{core}}{a_{core}+\Delta}\right)^4\right)\right\}, \qquad \frac{\Delta}{a_{core}} \gg 1 \tag{8b}$$

where

$$A_{core} = \frac{16\kappa_{shell}^4 - 12\kappa_{shell}^2 + \left(\frac{\alpha_{core}}{\alpha_{shell}}\right)^2\tau_{core}^2}{16\kappa_{core}^4 - 12\kappa_{core}^2 + \tau_{core}^2}\lambda \tag{9a}$$

$$A_{shell} = \frac{16(1+\tau_{shell}^2)\kappa_{shell}^4 - 8\kappa_{shell}^2\tau_{shell}^2 + \tau_{shell}^4}{3(16\kappa_{shell}^4 - 12\kappa_{shell}^2 + \tau_{shell}^2)} \times \frac{3 - 4\kappa_{core}^2 - \lambda(3-4\kappa_{shell}^2)}{3 - 4\kappa_{core}^2 + 4\lambda\kappa_{shell}^2} \tag{9b}$$

and τ satisfies the homogeneous eigenvalue equation

$$\tau\cot\tau = 1 - \frac{\tau^2}{4\kappa^2} \tag{10}$$

where the subscripts "core" and "shell" refer to values in the core and shell, respectively, as before.

A comparison of the exact solution with the asymptotic formulas, for Au@Pb core−shell particles, as used in ref 8, is given in Figure 1a. Similar results for Au@SiO_2 particles are given in Figure 1b, since these particles are also used commonly in practice. From these two figures, it is evident that the asymptotic formulas eq 8 accurately predict the vibrational frequencies within their respective regimes of validity. Interestingly, the precise regimes of validity of these formulas depend strongly on the materials of the core−shell particles, as is evident from Figure 1. By varying the material and geometric properties of the particles, in general it was found that the asymptotic formula eq 8a is accurate to within 5% if $\Delta/a_{core} < 0.3$, whereas eq 8b is accurate to within 5% if $\Delta/a_{core} > 1.5$. Given the complexity of the exact eigenvalue equation, we expect these formulas to prove useful in the design and characterization of core−shell nanoparticles.

Kinetics of Shell Formation. We now examine the kinetics involved in synthesizing the Au@Pb nanoparticles in Ref 8. In so doing, we give an a priori estimate for the lead shell thickness of the Au@Pb nanoparticles. Our calculations suggest that the actual thickness of the lead shell is less than that predicted in ref 8. Reasons for this shall be detailed.

In ref 8, lead-coated gold particles were synthesized following the process described by Mulvaney et al.[11] In this process, radiolytically generated radicals are produced homogeneously within a solution containing gold seed particles and free lead ions. The radicals transfer electrons to the core gold particles, and this leads to the deposition of lead onto the gold seeds via electrochemical reduction at the particle surface. Importantly, however, direct nucleation of free lead and, thus, formation of

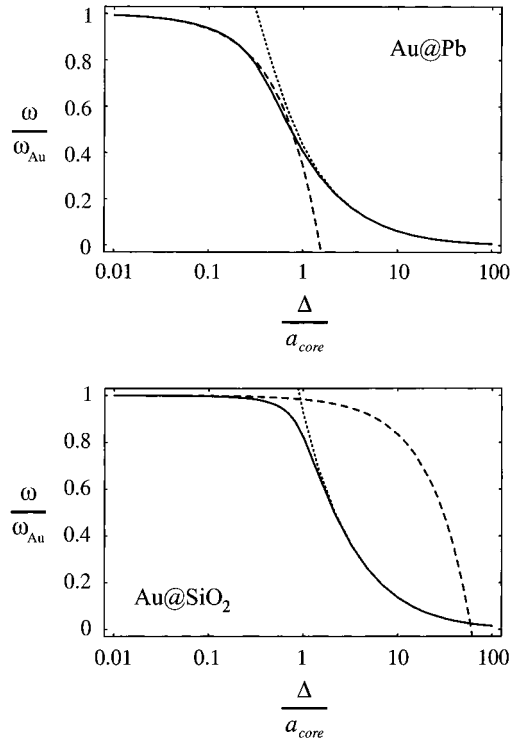

Figure 1. Ratio of breathing mode frequency ω for a core−shell sphere to that of a pure Au sphere ω_{Au}, with identical core radius, as a function of shell thickness Δ. Shell thickness Δ is normalized with core radius a_{core}. Exact solution (solid line); asymptotic formula eq 8a (dashed line); asymptotic formula eq 8b (dotted line). Material properties: Au [α = 3240 m/s, β = 1200 m/s, ρ = 19 320 kg m^{-3}]; Pb [α = 2160 m/s, β = 700 m/s, ρ = 11 340 kg m^{-3}]; SiO_2 [α = 5968 m/s, β = 3764 m/s, ρ = 2200 kg m^{-3}]. (a) Au@Pb sphere; (b) Au@SiO_2 sphere.

pure lead particles is also feasible if there are insufficient gold seed particles or the kinetics of electron transfer to the gold seeds are too sluggish. This may lead to an overestimate for the lead shell thickness if it is assumed that all the lead deposits onto the gold particles, as was done in ref 8.

To analyze the chemical process involved in the formation and deposition of lead specified in ref 8, we begin with the chemical reactions involved in the process. These may be summarized as follows:

$$\text{(a) } H_2O \xrightarrow{\gamma\text{-radiolysis}} (CH_3)_2COH$$

$$\text{(b) } (CH_3)_2COH + Au_n \xrightarrow{k_{et}} (CH_3)_2CO + H^+ + Au_n^-$$

$$\text{(c) } Pb^{2+} + Au_n^{2-} \rightarrow Au_nPb$$

$$\text{(d) } (CH_3)_2COH + Pb^{2+} \xrightarrow{k_1} Pb^+ + (CH_3)_2CO + H^+$$

$$\text{(e) } 2Pb^+ \xrightarrow{k_2} Pb + Pb^{2+}$$

$$\text{(f) } Pb^+ + Au_n^- \xrightarrow{k_3} Au_nPb$$

Radiolysis of water in the presence of 2-propanol produces $(CH_3)_2COH$ radicals,[11] reaction a. These either transfer electrons to the gold particles (reaction b), which leads to lead deposition via reaction c, or they directly reduce Pb^{2+} ions in solution, which causes the formation of separate lead particles via reaction e. The steady-state approximation can be applied to the radicals to evaluate the branching ratio between seeded growth (reaction c) and nucleation (reactions d and e):

TABLE 1: Lead Deposition Parameters for Au@Pb Nanoparticles with Au Core Sizes 7.5 and 23.5 nm, for the Experiments Conducted in refs 11 and 8, Respectively

	Au@Pb ref 11	Au@Pb ref 8	ref
Au core radius (nm)	7.5	23.5	11,8
radical generation rate (nM s^{-1})	133	133	11,8
[$HAuCl_4$] (mM)	0.50	0.50	11,8
[$Pb(ClO_4)_2$] (mM)	0.10	0.50	11,8
[Au_n] (nM)	4.85	0.128	11,8
steady state [Pb^+] (nM)	0.0244	2.54	this work
k_1 (M^{-1} s^{-1})	3×10^4	3×10^4	13
k_{et} (M^{-1} s^{-1})	5.7×10^{10}	1.8×10^{11}	this work
k_2 (M^{-1} s^{-1})	8.2×10^9	8.2×10^9	14
k_3 (M^{-1} s^{-1})	1.2×10^{10}	3.6×10^{10}	12

$$\frac{d[R]}{dt} = G - k_{et}[Au_n][R] - k_1[R][Pb^{2+}] = 0 \qquad (11)$$

where R denotes $(CH_3)_2COH$, G is the radical generation rate (M s^{-1}), [Au] is the gold colloid particle concentration, and k_{et} is the rate constant for electron transfer to the gold particles and is known to be close to the diffusion-limited rate constant of $k_{et} = 4\pi a_{Au} D N_a/1000$ (M^{-1} s^{-1}), where D is the radical diffusion coefficient of 10^{-5} cm^2 s^{-1}, N_a is Avogadro's Number, and a_{Au} is the gold particle radius. From eq 11, it is readily seen that the fraction Φ_1 of primary radicals that actually reacts with the seed, via reaction b, is given by

$$\Phi_1 = \frac{k_{et}[Au_n]}{k_1[Pb^{2+}] + k_{et}[Au_n]} \qquad (12)$$

Henglein and co-workers[12] have shown that a small number of Pb^+ radicals can subsequently be scavenged by metal colloids (reaction f) in competition with reaction e. A steady-state analysis of this secondary pathway reveals that the fraction Φ_2 of the Pb^+ radicals that can be scavenged in this way is given approximately by

$$\Phi_2 = \frac{k_3[Pb^+][Au_n]}{k_3[Pb^+][Au_n] + k_2[Pb^+]^2} \qquad (13)$$

From eqs 12 and 13 we then find that the total fraction Φ_{dep} of lead atoms that actually deposit onto the gold particles is

$$\Phi_{dep} = \Phi_1 + \Phi_2(1 - \Phi_1) \qquad (14)$$

Consequently, for a given lead concentration, the total radius of the particle a_{total} can be calculated a priori using

$$a_{total} = a_{core}\left(\Phi_{dep}\frac{V_m(Pb)[Pb^{2+}]}{V_m(Au)[Au_n]} + 1\right)^{1/3} \qquad (15)$$

where V_m(Pb) is the molar volume of lead metal and V_m(Au) is the molar volume of gold metal.

Inserting known values for the rate constants, listed in Table 1, we see that only a fraction $\Phi_1 = 0.61$ of primary radicals will result in deposition in the experiments of ref 8, compared to $\Phi_1 > 0.99$ in the original synthesis.[11] Furthermore, we find that the secondary pathway gives $\Phi_2 = 0.14$, indicating that 14% of the Pb^+ radicals are scavenged by the gold particles. Combining this latter result with the primary pathway, we find from eq 14 that the total fraction Φ_{dep} of lead deposited onto

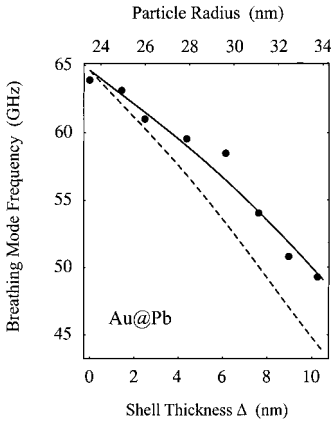

Figure 2. Comparison of experimental measurements (dots) to theoretical calculations (lines) of the breathing mode frequency of Au@Pb nanoparticles for various Pb shell thicknesses. Au core radius is 23.5 nm, and material properties are as given in Figure 1. Calculations including Pb shell thickness correction (solid line) and no thickness correction (dashed line).

the gold particles is $\Phi_{dep} = 0.66$, compared with >0.995 in the original synthesis.[11] This indicates that the lead shell thicknesses calculated in ref 8 overestimate the true experimental values.

Comparison with Experiment and Discussion

In Figure 2, we compare the experimental measurements for the Au@Pb particles in ref 8 with the above theoretical model. Two theoretical curves are presented: one assumes that all the lead deposits on the gold particles (as in ref 8), and a second includes the Pb shell thickness correction given in eq 15. Note the excellent agreement between theory and experiment when the Pb shell thickness correction is included, which predicts that the actual shell thickness is less than that assumed in ref 8, assuming that all the lead deposits on the gold results in an overestimate of the frequency shift. It is important to note that in the theoretical results presented, bulk values for material properties of Au and Pb are used. Although the validity of such an approach is questionable, given the small dimensions of the particles, the results in Figure 2 indicate that it is accurate. A more detailed comparison, with a range of different sized particles composed of different materials, needs to be performed before a general conclusion on its validity can be rigorously established. Nonetheless, taken together with results for nanoparticles composed of single materials,[2,3] these results indicate that models based on bulk continuum approaches can accurately describe the vibrational modes of nanometer sized particles.

Conclusions

We have presented a theoretical model for the acoustic breathing modes of core−shell spheres consisting of two materials with homogeneous, isotropic, and elastic properties. This included a kinetic analysis of the process used by Hodak et al.[8] to produce the Au@Pb nanoparticles. This kinetic analysis revealed that significant nucleation of free Pb particles occurred in these experiments,[8] which in turn reduced the amount of Pb deposited onto the Au seed particles. This combined model was compared to experimental measurements by Hodak et al.[8] on Au@Pb nanoparticles, where it was found to predict their behavior accurately. The analysis confirms that the frequency changes observed by Hodak et al.[8] are indeed due to the bimetallic nature of the particles.

The fundamental implications of these results can be summarized as follows. First, pulsed laser excitation of Au@Pb nanoparticles indeed launches the breathing mode in the core−shell particle. It would be interesting to establish if the same mode is excited when either the core or the shell is selectively excited. This could be achieved in an ultrafast experiment with core−shell particles composed of metals and dielectrics. For example, one could employ $Au@SiO_2$ particles. In such experiments, a visible/near-UV pulse could be used to selectively excite the metal core, which will launch the acoustic vibrational mode before any significant heat transfer to the dielectric occurs. Such experiments are currently underway. Second, it was found that the Au core and Pb metal shell behave like bulk materials in the excitation of the breathing mode, despite their small dimensions. A more detailed comparison between theory and experiment needs to be performed to establish a definite conclusion.

Acknowledgment. This research was supported in part by the Particulate Fluids Processing Centre of the Australian Research Council and by the Australian Research Council Grants Scheme. The authors would like to thank A/Prof. B. D. Hughes for many interesting and stimulating discussions. P. Mulvaney also thanks the Humboldt Foundation for support, and the staff at the Max-Planck Institute for Colloids and Surfaces for their hospitality.

References and Notes

(1) Duval, E.; Boukenter, A.; Champagnon, B. *Phys. Rev. Lett.* **1986**, *56*, 2052.
(2) Hodak, J. H.; Henglein, A.; Hartland, G. V. *J. Chem. Phys.* **1999**, *111*, 8613−8621.
(3) Hodak, J. H.; Henglein, A.; Hartland, G. V. *J. Phys. Chem. B* **2000**, *104*, 9954−9965.
(4) Lamb, H. *Proc. London Math. Soc.* **1882**, *13*, 189.
(5) Hines, M. A.; Guyot-Sionnest, P. *J. Phys. Chem.* **1996**, *100*, 468.
(6) Liz-Márzan, L. M.; Giersig, M.; Mulvaney, P. *Langmuir* **1996**, *12*, 4329−4336.
(7) Mulvaney, P. *Langmuir* **1996**, *12*, 788−801.
(8) Hodak, J. H.; Henglein, A.; Hartland, G. V. *J. Phys. Chem. B* **2000**, *104*, 5053−5055.
(9) Bullen, K. E. *An Introduction to the Theory of Seismology*; Cambridge University Press: Cambridge, 1963.
(10) Inclusion of the effects of the surrounding fluid has negligible effect on the dynamics of vibration.
(11) Mulvaney, P.; Giersig, M.; Henglein, A. *J. Phys. Chem.* **1992**, *96*, 10419−10424.
(12) Henglein, A.; Holzwarth, A.; Janata, E. *Ber. Bunsen-Ges. Phys. Chem.* **1993**, *97*, 1429−1434.
(13) Breitenkamp, M.; Henglein, A.; Lilie, J. *Ber. Bunsen-Ges. Phys. Chem.* **1976**, *80*, 973−979.
(14) Henglein, A.; Janata, E.; Fojtik, A. *J. Phys. Chem.* **1992**, *96*, 4734−4736.